Available online at www.CivileJournal.org

Civil Engineering Journal

(E-ISSN: 2476-3055; ISSN: 2676-6957)

Vol. 12, No. 03, March, 2026

Synergistic Effects of Nano Titanium Dioxide and Nano Zinc Oxide on the Physical and Rheological Properties of Asphalt Binder

Hadel Obaidi [1*], Hussein K. Mohammad [2], Amjad H. Albayati [1]

[1] *Department of Civil Engineering, University of Baghdad, Baghdad 17001, Iraq.*

[2] *Ministry of Higher Education and Scientific Research, Baghdad 10072, Iraq.*

Received 16 December 2025; Revised 19 February 2026; Accepted 24 February 2026; Published 01 March 2026

Abstract

Enhancing asphalt binder performance against anticipated distresses is a critical focus in pavement engineering. This study investigates the synergistic influence of nano titanium dioxide (NT) and nano zinc oxide (NZ) on asphalt binder performance. Nine NT:NZ combinations (1:1 to 3:3) were prepared with 1–3% by binder weight, in addition to a reference binder (RB). The performance test program included; conventional tests (penetration, softening point, viscosity, and ductility), Dynamic Shear Rheometer (DSR) for performance grading, Multiple Stress Creep Recovery (MSCR) for rutting evaluation, and Linear Amplitude Sweep (LAS) for fatigue resistance. Furthermore, Statistical analysis (ANOVA) was performed to determine the significance of nanomaterial interactions, and a cost–performance evaluation assessed economic feasibility. The results revealed that the combined use of these types of NM increased binder stiffness and resistance to aging. Additionally, the high-temperature PG grade increased from 70°C to 76°C for all NM-modified asphalt binders, except for the combinations of 1% NT and 1% NZ, as well as the (1:2) binder. On the other hand, MSCR results showed a reduction of up to 32% in non-recoverable creep compliance (Jnr3.2), whereas the LAS test verified extended fatigue life at a 2.5% strain level for low dosages of the NM combination, i.e., (1:1). The 1:1 NT:NZ blend exhibited the highest cost–performance efficiency, providing a balanced improvement in rutting and fatigue resistance. Overall, the synergistic incorporation of NT and NZ significantly enhanced the binder performance, offering practical insights for selecting nanomaterials in sustainable pavement engineering.

Keywords: Nanomaterials; Titanium Dioxide; Zinc Oxide; MSCR; LAS.

1. Introduction

Asphalt binder is an essential element of asphalt concrete; its behavior is strongly influenced by aging and environmental conditions. These play a major role in determining pavement endurance and overall performance [1, 2]. As the binder's properties directly affect rut resistance, fatigue cracking, and long-term durability, modifying the asphalt binder has become a widely adopted strategy to improve pavement performance [3-5].

In recent years, Nanomaterials (NM) have gained considerable attention as advanced modifiers, largely due to their extremely high surface area, chemical activity, and ability to improve the physical and rheological properties of asphalt binder materials [6-9]. Many research have investigated the use of NM in asphalt concrete, reporting improvement in stiffness, viscosity, elasticity, and resistance to deformation and fatigue [10, 11]. Among the various nanomaterials explored, titanium dioxide (TiO_2) and zinc oxide (ZnO) have shown particularly promising results owing to their chemical stability, low toxicity, and strong resistance to ultraviolet (UV) radiation [12]. TiO_2 has drawn significant

* Corresponding author: hadel.i@coeng.uobaghdad.edu.iq

https://doi.org/10.28991/CEJ-2026-012-03-013

interest in terms of its mechanical and durability properties in addition to its photocatalytic ability. This property supports the development of environmentally eco-active pavement capable of reducing air pollution. In addition to these advantages, TiO_2 can absorb ultraviolet radiation, helping to reduce oxidative aging while increasing viscosity, hardening, and softening point that enhance permanent deformation resistance at high temperatures [13, 14].

Similarly, ZnO nanoparticles provide strong UV-shielding capacity and high thermal conductivity, which help to slow aging in asphalt binders and strengthen binder-aggregate adhesion. Recent studies suggest that ZnO can enhance stiffness and viscosity, extend fatigue life, and improve mechanical performance at low temperatures, providing a more balanced performance improvement compared to some other nano modifiers [15-18].

Table 1 provides an overview of earlier research that used TiO_2 and ZnO in asphalt binders, outlining the dosage ranges examined and the main effects reported. Most of these studies have focused on individual nanomaterials which in turn confirm potential improvements within physical and rheological characteristics of asphalt binder that still lack a limited insight into their combined behavior.

Table 1. Outline of previous research on TiO_2 and ZnO nanoparticles used in asphalt binders

Material	Researcher	Dosage	Main Finding
Nano TiO_2	Tanzadeh et al. (2013) [19]	4%	- Enhanced rutting resistance of the asphalt mixture. - Improved temperature susceptibility of the modified binder.
	Buhari et al. (2018) [20]	2, 4, 6, 8, 10%	- At nano TiO_2 contents of up to 10%, the nanomodified binder exhibited significant improvements in workability, stiffness, and elasticity
	Qian et al. (2019) [21]	1, 2, 5, 10%	- 5% nano TiO_2 improved high-temperature rutting resistance and demonstrated effective NO_2 degradation through photocatalytic action.
	Cadorin et al. (2021) [22]	3%, 6%, 9%, 12%, and 15%	- Increasing TiO_2 content enhanced stiffness, rutting, fatigue, and aging resistance without compromising rheological properties, although NO_x degradation efficiency remained limited.
	Ameli et al. (2020) [23]	2, 4, 6, 8%	- Nano TiO2 enhanced the rutting and fatigue resistance properties.
	Weigel et al. (2020) [24]	10%	- FTIR analysis confirmed that TiO_2 positively modified the aromatic C–H chains and influenced structural rearrangement at higher temperatures, promoting asphaltene extension. This behavior suggests that TiO_2 acts both as a filler and as an effective anti-aging modifier
	Aboelmagd et al. (2021) [25]	1, 3, 5, 7%	- The addition of 5% nano TiO_2 to asphalt improved viscosity, rutting resistance, and fatigue life
	Filho et al. (2022) [26]	3%	- Oleylamine-modified TiO_2 improved fatigue life, deformation resistance, and aging properties.
	Enieb et al. (2023) [27]	1.5, 3.5, 5.5, 9%	- TiO_2 significantly improved the physical and rheological properties of 60/70 asphalt binder, increasing stiffness, reducing Jnr in MSCR tests, and decreasing rut depth in Hamburg Wheel tracking.
	Mohammed & Abed (2024) [28]	1, 3, 5, 7%	- 5% TiO_2 has promoted binder physical and rheological property and sustains anti-rutting and fatigue criteria.
	Albayati et al. (2024) [29]	2, 4, 6, 8%	- An optimal TiO_2 dosage of 6% achieved uniform dispersion within the binder, enhancing thermal and oxidative stability, increasing stiffness and Marshall stability, and reducing moisture damage and rutting depth by up to 84% and 64%, respectively.
Nano ZnO	Zhang et al. (2018) [30]	2, 3, 4%	- Reducing ZnO particle size from 2 mm to 80 nm slightly affected penetration and softening point while improving ductility. The rutting factor (G/sin δ) increased by approximately 22%, 36%, and 9% with each ZnO increment, showing minimal influence on low-temperature stiffness and creep behavior.
	Yunus et al. (2018) [31]	3, 5, 7%	- Nano ZnO led to increased asphalt stiffness, decreased penetration, raised softening point, and greatly improved rutting resistance.
	Saltan et al. (2019) [32]	1, 3, 5%	- Up to 5% ZnO yielded uniform dispersion (~4 μm agglomerates), enhancing penetration, softening point, viscosity, and rutting resistance, while 1% ZnO showed higher aging and thermal cracking susceptibility.
	Xu et al. (2019) [33]	1.0–5.0%	- The optimal ZnO content was identified at 3%, providing over 95% UV absorption and improving penetration and softening point values. However, excessive ZnO slightly reduced G*, indicating limited enhancement in rutting and fatigue resistance beyond this level.
	Kleizienė et al. (2019) [34]	1, 3%	- Enhanced permanent deformation resistance. - Excessive dosage may reduce fatigue resistance.
	Neto et al. (2022) [35]	3, 5, 7%	- Nano ZnO (7%) significantly improved the asphalt binder's Performance Grade (PG). - Proved technical feasibility.
	Kamboozia et al. (2022) [36]	2, 4, 6, 8%	- An optimal 6% ZnO increased bonding energy and viscosity within the asphalt matrix, reducing rutting depth by about 40.6% after repeated wheel loads under freeze–thaw cycles.
	Al-Mistarehi et al. (2023) [37]	1, 2, 3%	- Nano ZnO improved binder cracking resistance at lower temperature. - Increased flash and fire points, viscosity, and softening point.
	Melo et al. (2023) [38]	3, 6, 9, 12, 15%	- ZnO-modified binders exhibited improved aging resistance and increased stiffness, as shown by higher dynamic modulus and reduced non-recoverable compliance, enhancing rutting performance. However, at 15% ZnO, excessive stiffness increased stress amplitude in LAS tests, reducing fatigue resistance.
	Zhu et al. (2024) [39]	1, 3, 5%	- ZnO at nano range of 10-30 nm showed the greatest enhancements. - Improved asphalt's (PG 64-22) elasticity, rutting, anti-aging, and physical properties.

While TiO_2 and ZnO have each demonstrated significant potential, limited research has investigated their simultaneous incorporation and synergistic interactions within asphalt binders. For example, Fu [40] observed enhanced stability and deformation resistance when TiO_2 and ZnO were combined in fiber-reinforced asphalt mixtures, attributing this to uniform nanoparticle dispersion. Di et al. [41] also reported that dual NT–NZ modification improved aging and fatigue performance. Whereas Han et al. [42] found minimal improvements when these nanoparticles were introduced into SBS-modified binders. Such discrepancies highlight that the combined effects of TiO_2 and ZnO depend strongly on their proportion, dispersion, and interaction within the binder matrix. Therefore, this study aims to systematically investigate the synergistic influence of nano TiO_2 and nano ZnO on the physical, rheological, and durability characteristics of asphalt binders. Three dosages of each nanoparticle (1%, 2%, and 3% by binder weight) were evaluated, producing nine NT:NZ combinations and a reference binder. The experimental program encompassed conventional tests (penetration, softening point, viscosity, ductility, and storage stability), short-term aging (mass loss and aging indices), and rheological characterization using Dynamic Shear Rheometer (DSR), Multiple Stress Creep Recovery (MSCR), and Linear Amplitude Sweep (LAS) tests. This comprehensive approach enables the assessment of whether the dual incorporation of TiO_2 and ZnO produces synergistic improvements beyond those achievable by either nanomaterial alone.

2. Materials and Methods

2.1. Asphalt Cement

A penetration grade 40-50 asphalt binder, obtained from the Doura Oil Refinery in Baghdad, Iraq was used as the base material in this study. It was chosen to serve as the reference binder for the evaluation of the effects of nano-modification, representing a conventional binder that is frequently employed in pavement construction. The conventional properties of the binder were determined in accordance with ASTM D946 standards and summarized in Tables 2 and 3. In addition, its performance grade (PG) characteristics were evaluated following AASHTO M302, confirming a classification of PG 70–16.

Table 2. Conventional properties of asphalt cement

Test	Unit	ASTM designation	Result	Specification limit, ASTM D946
Penetration at 25°C, 100 gm., and 5 sec.	0.1 mm	ASTM D5	40	40-50
Softening point, ring and ball.	°C	ASTM D36	49	-
Specific gravity at 25°C.	-	ASTM D70	1.029	-
Flash point.	°C	ASTM D92	288	Min. 232
Ductility.	cm	ASTM D113	110	Min. 100
Residue from thin film oven test (ASTM D1754).				
Retained penetration, % of original.	%	ASTM D5	57.5	Min. 55
Ductility at 25°C, 5 cm/min.	cm	ASTM D113	60	Min. 25

Table 3. Rheological properties of asphalt cement

Asphalt cement	Properties	Temperature Measured (°C)	Results	Specification Requirements, AASHTO M320
	Viscosity at 135 °C (Pa.s)	-	720	3000 m Pa.s, max
	DSR, G/sinδ at 10 rad/s (kPa)	58	8.91	1.00 kPa, min
		64	3.82	
		70	1.77	
		76	0.86	
RTFO Aged	Mass Loss (%)	-	0.30	1%, max
	DSR, G/sinδ at 10 rad/s (kPa)	64	7.02	2.2 kPa, min
		70	3.65	
		76	1.85	
PAV Aged	DSR, G.sinδ at 10 rad/s (kPa)	28	3921	6000 kPa, max
		25	5324	
	BBR, Creep Stiffness (MPa)	-6	197	300 MPa, max
	Slope m-value	-6	0.336	0.3, min

2.2. Nanomaterials

In this study, a combination of two inorganic nanomaterials, NT and NZ, was employed to prepare nano-modified asphalt binders. Both nanomaterials were incorporated simultaneously at dosage levels of 1%, 2%, and 3% by total binder weight. Their physical appearance is shown in Figure 1, while their principal physicochemical properties are summarized in Table 4. The NT and NZ powders exhibited high purity (99.9%) and fine particle sizes within the nanometer range. The NT appeared as an off-white powder with a specific surface area of 80–120 m^2/g, whereas NZ appeared as a white powder with a surface area of 30–60 m^2/g. Both nanomaterials possess high melting points and excellent chemical stability under asphalt mixing conditions, enabling them to maintain their structural integrity during blending and testing.

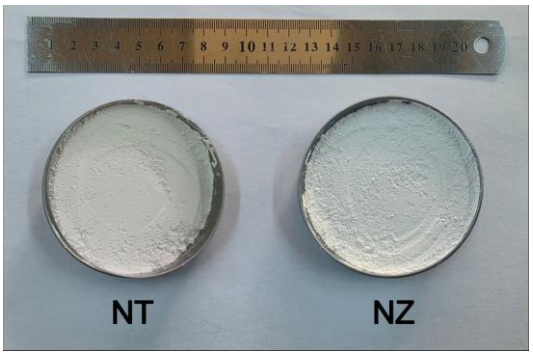

Figure 1. Physical appearance of nanomaterials

Table 4. Physical properties of nanomaterials

Properties	Nanomaterial	
	NT	NZ
Chemical Formula	TiO_2	ZnO
Molecular Wt. (g/mol)	85.42	81.39
Appearance	Off White Powder	White Powder
Mean particle size (nm)	20-30	15-20
Purity grade (%)	99.9	99.9
Surface area (m^2/g)	80-120	30-60
Melt temperature (°C)	1860	1975
Bulk density (g/mL)	0.51	0.331

To verify the particle size distribution, a granulation analysis was conducted using a Brookhaven Instruments 90Plus Particle Sizing Analyzer (Software Ver. 5.34). The results obtained (Figure 2) illustrate the intensity-based long-distance particle size distributions along with their corresponding cumulative distribution curves. The NT particles displayed a relatively broader distribution with an effective diameter around 24 nm, while NZ particles exhibited a narrower and finer size range centered around 17 nm. This confirms that both nanomaterials fall within the nanoscale region and possess adequate fineness for effective dispersion and interaction within the asphalt binder matrix.

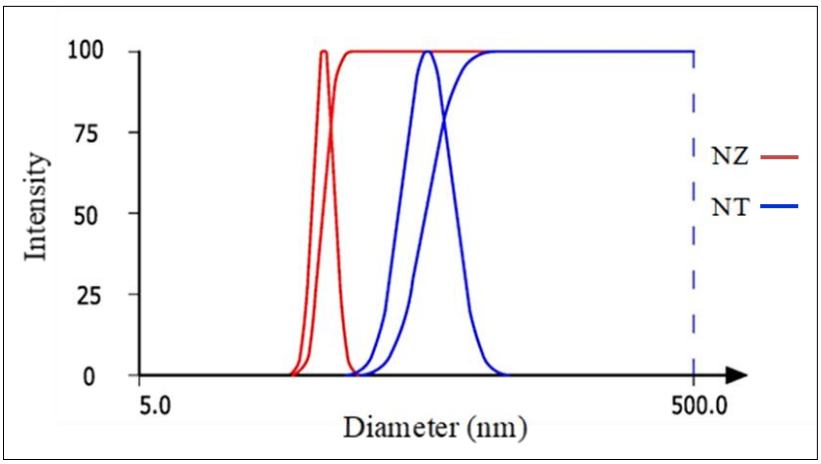

Figure 2. Lognormal particle size distribution of nanomaterials

The Scanning Electron Microscopy (SEM) was used to analyze the morphology of the nanoparticles at a magnification of 60,000×, as shown in Figure 3. The results of SEM of TiO_2 display a densely packed arrangement of mostly spherical particles, with moderate agglomeration forming compact clusters which is typical for TiO_2 nanoparticles. Moreover, the results of SEM of ZnO show that the particles were more angular and irregular shapes, slightly rough surfaces, and localized clumping. These distinctive morphological features correspond to the usual properties of metal oxide nanoparticles and provide important insight into their surface texture and dispersion characteristics before they are incorporated into the asphalt binder.

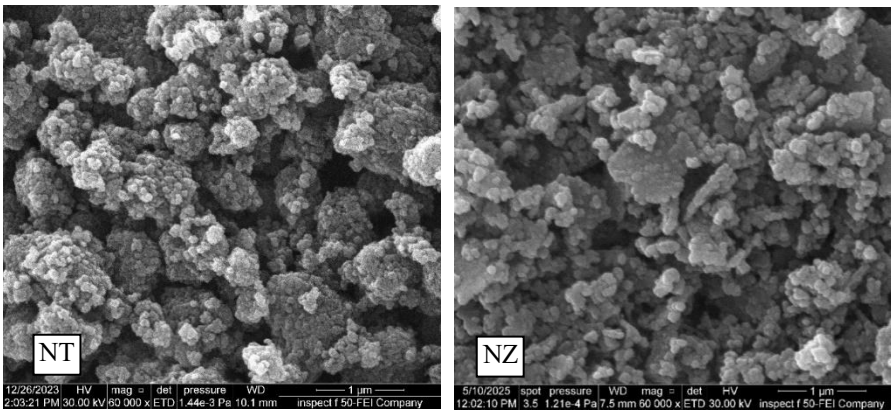

Figure 3. SEM for the Nanomaterials

2.3. Binder Preparation

The preparation of nano modified binder was done as per the method described by [43] with slight adjustment to suit the objective of this research, which was done at binder level using dry blending technique. At the beginning, RB binder was heated to a temperature of 150±1 °C to achieve a uniform fluidity for blending purposes. Then the heated binder was stirred using high speed shear mixer for 20 minutes at speed of 1000 rpm to ensure homogenization of the RB. After that, the NM, i.e. the NT as well as NZ were simultaneously introduced to the heated binder gradually at rate of 4 gm per minute to minimize the effect of nanoparticles agglomeration in the binder. During the addition, the binder was mixed using high speed shear mixer at a speed of 4000 rpm, the mixing procedure was continued after the completion of nanomaterial addition for a time of 30 minutes. A geometrical steel consists of jiffy shaped-mixing head (as shown in Figure 4.a) was introduced with shear mixer to disperse the nanoparticles during binder modification using 4 stages (rotation, centrifugal, intense shear and suction of particles in the binder matrix) employed to prevent possible development vortex and anticipated aging under the laboratory binder modification. The blending process was monitored closely by a thermal imaging camera (as shown in figure 4.b) to ensure uniform dispersion of nanomaterial and even distribution of temperature through the modified binder. Upon completion of blending, the modified binder was poured into a metal container and allowed to cool to room temperature before being sealed to store and for subsequent testing. For ease of referencing throughout the experimental results discussion, each blend is labeled using two parts notations, (I: II), where I indicate the percentage of NT while II denotes the NZ percentage. For example, an asphalt binder with 1 % NT and 1% NZ has a label of (1:1). The reference binder which is denoted as RB was used as a benchmark for results comparison. In total, nine nano-modified asphalt binders were prepared and evaluated in this study, corresponding to NT and NZ dosages of 1 %, 2 %, and 3 %. Furthermore, a workflow chart presented in Figure 5 describes the necessary steps for nanomodified binder preparing and testing of this study.

(a) **(b)**

Figure 4. a) Mixing head geometry, b) Thermal and visual monitoring of the mixing process

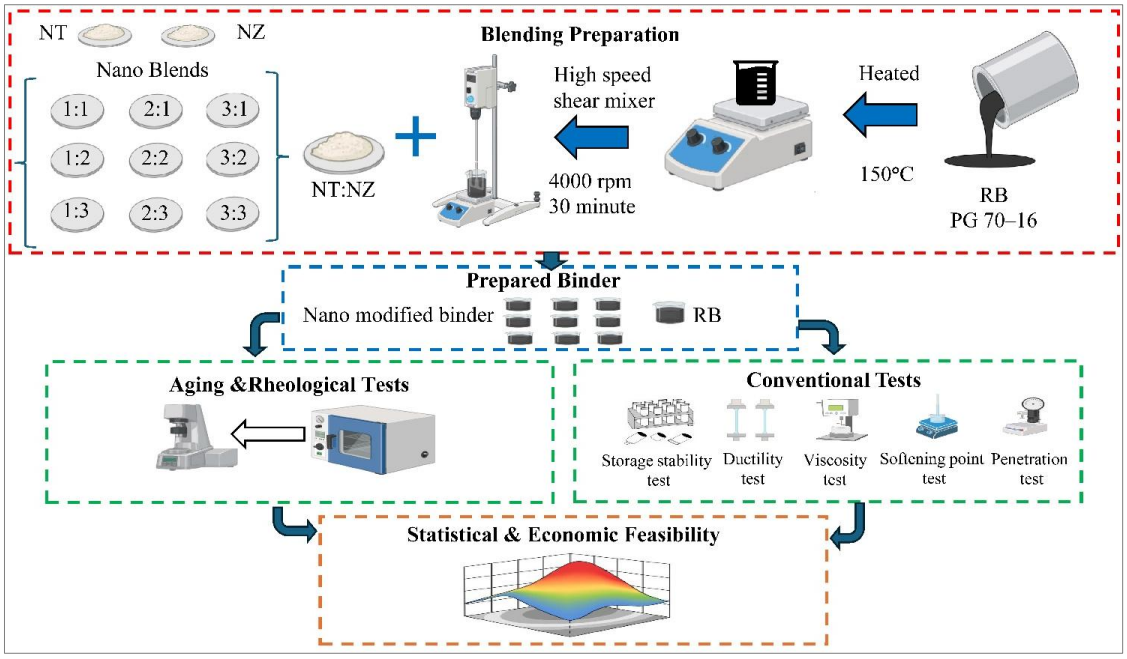

Figure 5. Workflow chart describes steps for preparation and testing of RB and nanomodified binder

2.4. Testing Program

2.4.1. Conventional Properties

The conventional properties using tests like penetration, softening point, rotational viscosity and ductility were conducted for the RB as well as the nano modified binders. To measure the consistency of asphalt binder, the penetration test was conducted as per the method described in ASTM D5 at a temperature of 25 °C with a standard needle under weight of 100 gm for 5 sec. The temperature susceptibility was evaluated using the softening point test as per the procedure outlined in ASTM D 36 using ring and ball apparatus to characterize the temperature at which the asphalt binder softens and is converted from a solid state to a liquid state. To evaluate the flow and workability behavior of asphalt binder, a rotational viscosity test was conducted as per the method described in ASTM D 4402 using a Brookfield viscometer with spindle #29 at a temperature of 135°C. The tensile properties assessment of different asphalt binder types, a ductility test was performed based on the procedure outlined in ASTM D 113 at a temperature of 25 °C. Finally, the tendency of NM to agglomeration and dispersion ability within the asphalt cement, storage stability was examined following ASTM D7173. Following this test method, asphalt binder samples were placed in aluminum tubes with dimensions of 14 cm length and 2.5 cm diameter and stored vertically at an oven with a temperature of 163 °C for 48 h. Then, the samples were cooled to −10 °C and the tube samples were sectioned into top and bottom portions. The softening point for samples belonging to the top and bottom sections performed and the difference between them recorded indicating the potential of nanoparticle agglomeration and dispersion.

2.4.2. Aging Performance

To investigate the effect of both NT and NZ nano modified asphalt binder on the aging performance, Rolling Thin Film Oven test (RTFO) following ASTM 2872 was conducted to mimic the thermal and oxidative conditions experienced during asphalt binder production in the mix plant. The aging condition is represented by keeping the asphalt binder at 163°C for 85 minutes with 4 L/min airflow. After which, the percentage mass loss of each asphalt binder sample was measured to evaluate the extent of volatilization and oxidation caused by aging. Also, to examine the effect of nanomaterial on the aged asphalt sample properties in comparison to those of the original condition, Aging Index (AI) was calculated for the following test penetration, rotational viscosity, and softening point. These indices quantify the changes in binder properties due to aging. The AI values above one indicates increased stiffness and reduced flexibility. The AI was calculated as per the following equations:

$$\mathrm{AI}_{Pen} = \frac{Pen_{(unaged)}}{Pen_{(RTFO)}} \quad (1)$$

$$\mathrm{AI}_{SP} = \frac{SP_{(RTFO)}}{SP_{(unaged)}} \quad (2)$$

$$\mathrm{AI}_{Visc} = \frac{Visc_{(RTFO)}}{Visc_{(unaged)}} \quad (3)$$

where, the Pen, SP and Visc with nomination of (unaged) refer to the penetration, softening point and rotational viscosity values, respectively, for the unaged samples (original condition) whereas those denoted as (RTFO) refer to the corresponding values after RTFO aging.

2.4.3. High-Temperature PG Grade

Dynamic shear rheometer (DSR) type Anton Paar (Smartpave 102e) was used to assess the high temperature PG for the unaged samples following AASHTO T315. The binder's viscoelastic behavior and their resistance to permanent deformation were assessed through rutting parameter (G*/sin δ) at a fixed frequency of 10 rad/sec. and strain level of 12%, to ensure that the asphalt binder within the linear viscoelastic range. The starting temperature of the test was 58°C and increased in intervals of 6°C each time the binder passed the limit of 1 kPa for the rutting parameter. The test continued until the value fell below the limit and the highest temperature at which this criterion was met is taken as the binder's high-temperature PG grade, indicating its stiffness and resistance to rutting under elevated service conditions.

2.4.4. MSCR Test

The Multiple stress creep recovery test was conducted following the procedure outlined in AASHTO T350 at a temperature of 70°C (corresponding to high temperature PG of RB binder) to assess the resistance to permanent deformation of asphalt binder. The RTFO aged samples were subjected to 30 cycles of shear stressing, including 10 preconditioning cycles at a low stress level of 0.1 kPa, followed by ten cycles at the same stress level and ten at a stress level of 3.2 kPa. Each cycle included a 1 second creep loading followed by 9 seconds strain recovery intervals, applied continuously. During the test, the shear strain response (ε) continuously recorded to determine the peak strain (εp), the recovered strain (εr), and the non-recoverable strain (εnr), as shown in the schematic diagram for the test presented in Figure 6.

Based on the test measurements, two key parameters were calculated: the percent recovery (%R) and the non-recoverable creep compliance (J_{nr}), using the following equations:

$$\%\, R = \frac{\varepsilon_r}{\varepsilon_p} \times 100 \tag{4}$$

$$J_{nr} = \frac{\varepsilon_{nr}}{\tau} \tag{5}$$

These parameters provide a quantitative measure of the binder's elastic recovery and its capacity to resist permanent deformation under repeated high-temperature loading.

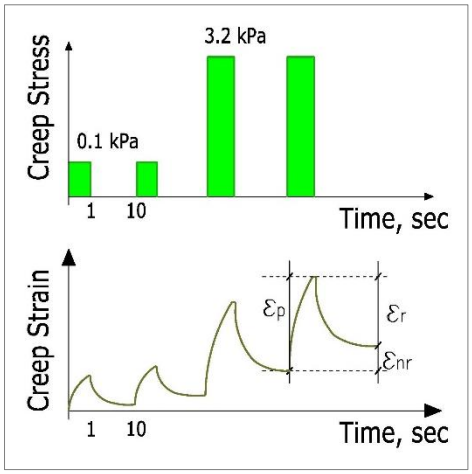

Figure 6. Schematic presentation for MSCR test

2.4.5. LAS Test

The fatigue performance of the asphalt binders was evaluated using the Linear Amplitude Sweep (LAS) test in accordance with AASHTO T391. Binder specimens exposed to aging by using the Rolling Thin Film Oven (RTFO) and the Pressure Aging Vessel (PAV) were tested with an 8 mm parallel plate geometry and a 2 mm gap. These tests were carried out at 25 °C, representing typical intermediate in-service conditions of pavement.

The test procedure of LAS includes a frequency sweep followed by an amplitude sweep. During the frequency sweep, an oscillatory shear strain of 0.1% implemented across a frequency range of 0.2–30 Hz to illustrate the properties of undamaged viscoelastic behavior of the asphalt binder. The parameter used to determine the undamaged material was (α).

According to the subsequent amplitude sweep, the shear strain amplitude was increased linearly from 0 to 30% at a constant frequency of 10 Hz corresponding to approximately 3,100 loading cycles.

This result simulates the progressive accumulation of fatigue damage under repeated loading, as illustrated in Figure 7. According to the amplitude sweep, main parameters included peak shear strain, peak shear stress, phase angle (δ) and complex shear modulus (G*) continuously monitored. Fatigue life (Nf) was predicted using the model of viscoelastic continuum damage (VECD) by the following relationship:

$$Nf = A(\Upsilon max)^{-B} \quad (6)$$

The maximum expected strain (γ_{max}) represents the strain experienced by the pavement. The parameter (A) represents the binder damage parameter collected from the amplitude sweep phase, while (B) represents the slope derived from the properties of undamaged material (B = -2α).

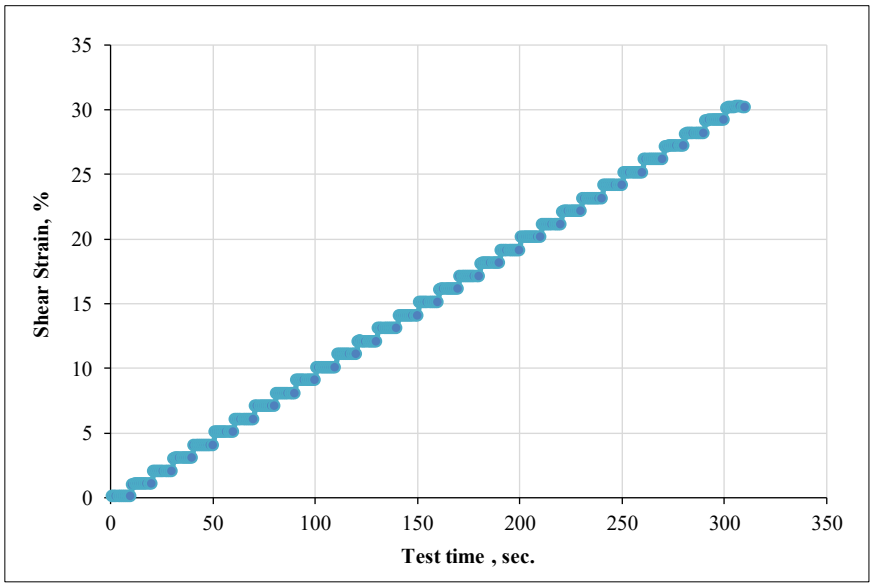

Figure 7. Schematic illustration of the amplitude sweep loading protocol

2.5. Statistical Analysis

The results obtained from all experimental tests were analyzed statistically using analysis of variance (ANOVA) to determine the significance of observed variations among different binder types. Each reported value represents the mean of three replicate measurements for each blend to ensure result reliability and minimize experimental variability. Both single-factor and two-way ANOVA models were employed to evaluate the main effects of NT and NZ, as well as their combined interaction (NT × NZ), which reflects the potential synergistic influence of the two nanomaterials. A 95% confidence level was chosen for the analysis, where a p-value less than 0.05 indicates a statistically significant difference in the dependent variables, leading to the rejection of the null hypothesis. All statistical computations were carried out using Minitab software (Version 17).

3. Results and Discussion

3.1. Results of Conventional Properties

The effects of NT and NZ on the conventional properties of asphalt binders are illustrated in Figures 8-12. The incorporation of these nanomaterials led to significant changes in binder properties, with the extent of the effect depending on the type and dosage of nanoparticles.

From Figure 8, the results of the penetration test presented a gradual reduction in the values of penetration with increasing nanoparticle content thus rising in binder stiffness. The values of penetration of the RB decreased by approximately 50% with (3:3) NT:NZ blend. Statistical analysis confirmed that the combined NT×NZ factor had a significant effect on penetration ($p = 0.014$), demonstrating that the synergistic addition of TiO_2 and ZnO nanoparticles can effectively increases the binder stiffness. This reduction in penetration is attributed to the enhanced internal cohesion and restricted molecular mobility caused by the uniform dispersion of nanoparticles within the binder matrix. These findings are consistent with those reported in [27, 34], which presents a similar improvement at level of nanoparticle-induced reinforcement and increased intermolecular friction within the asphalt structure.

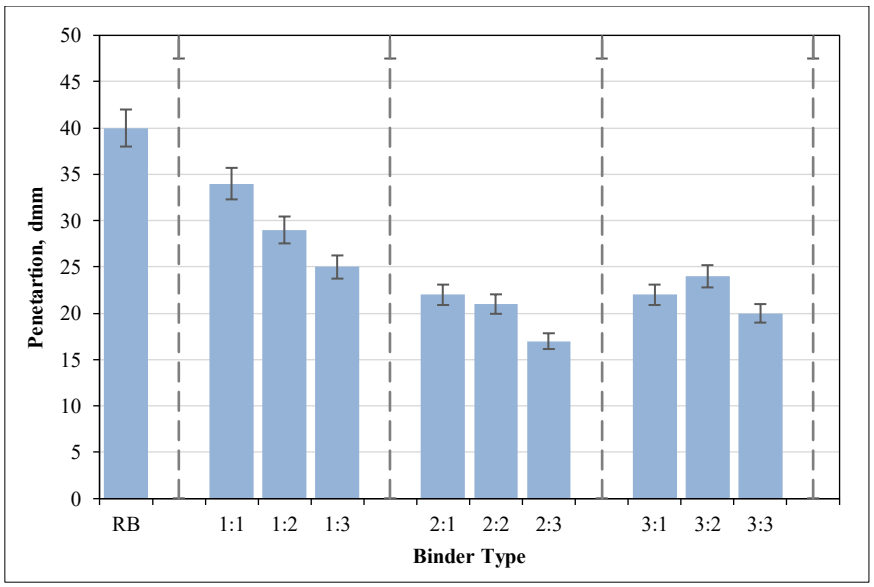

Figure 8. Penetration values with different types of binder

From Figure 9, the results of the softening point test show a consistent increase with higher nanoparticle content, indicating improved thermal stability of the modified binders. The NT:NZ blends (1:3), (2:3), and (3:3) exhibited the highest softening point values, approximately 11–12% higher than the RB. This trend suggests that increasing the proportion of ZnO in the mixture enhances the binder's resistance to thermal deformation. The statistical analysis confirmed that the combined NT×NZ interaction had a significant effect on softening point ($p = 0.023$), supporting the existence of a synergistic influence between the two nanomaterials. However, the increase in softening point was more strongly associated with ZnO content, as mixtures containing higher NZ ratios consistently demonstrated superior performance compared to those with higher NT content. This behavior can be attributed to ZnO's higher thermal conductivity and strong UV-shielding capability, which slow down heat-induced softening and oxidative degradation. These findings were agree with [40, 41] who reported that NZ improves thermal resistance of binder leading to a more effective than NT.

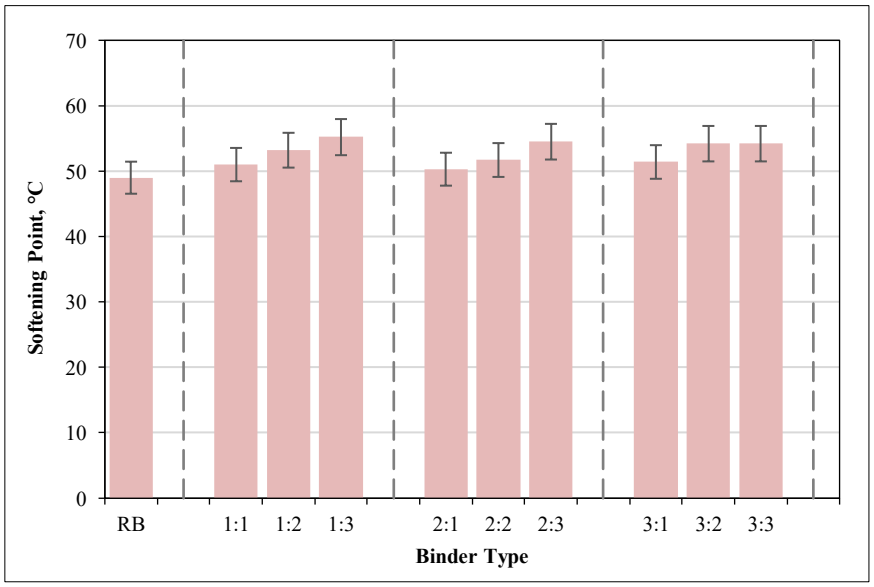

Figure 9. Softening points with different types of binder

According to Figure 10, the rotational viscosity of the binders increased markedly with the incorporation of nanoparticles, indicating improved internal consistency and shear resistance. The viscosity of the (3:3) NT:NZ blend was approximately 81.5 % higher than that of the (RB, confirming the significant stiffening effect of nanoparticle addition. ANOVA result verified that the combined NT×NZ interaction had a highly significant influence on viscosity ($p = 0.0003$), reflecting the synergistic role of those two nanomaterials in enhancing binder resistance to flow. Examination of the viscosity trend shows that increasing the proportion of NZ at a fixed NT level, such as in the 1:1 → 1:3 and 2:1 → 2:3 sequences, consistently resulted in higher viscosity values, suggesting that NZ exerts a more pronounced effect than NT. This behavior may be attributed to the higher surface activity of ZnO's and better interfacial

bonding within the asphalt matrix, which enhances energy dissipation under shear. Despite these increases, all viscosities remained well below the Superpave upper limit of 3000 mPa·s, ensuring adequate pumpability and workability during mixing and compaction. Similar conclusions were reported by [23, 29] indicating that nanomodified binders exhibit improved viscosity and structural stability without compromising workability.

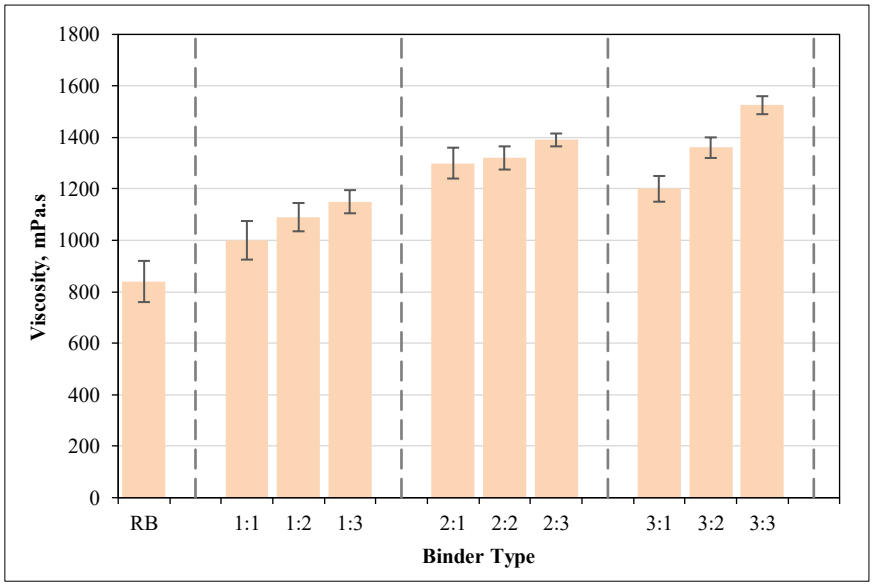

Figure 10. Rotational viscosities with different types of binder

From Figure 11, the ductility results showed a consistent decrease with increasing nanoparticle content, reflecting the expected trade-off between binder stiffness and flexibility. This response would link to enhance performance in hot climate weather (besides decrease penetration value and increase viscosity) to address premature failure of rutting issues. In contrast, diminish binder tensile extendibility at lower temperatures by means of gained stiffness. Thus, increasing susceptibility to fatigue induces cracking as well as pavement life. However, the complicated interaction between nano and asphalt binder may suggest that tensile ductility value may not be standalone to assure binder at lower temperature, so LAS test may cover this behavior. The largest reduction, approximately 30% compared to the RB, observed for the (3:2) and (3:3) NT:NZ blends containing higher NT proportions. Statistical analysis confirmed that the combined NT×NZ interaction had a significant effect on ductility ($p = 0.003$), indicating that nanoparticle incorporation collectively increased stiffness and reduced elongation capacity. This behavior is attributed to restricted molecular mobility and limited chain elongation under tensile stress due to the formation of a denser nanoparticle network within the binder matrix. Although the 1:1 binder-maintained ductility slightly above the 100 cm specification limit, all other modified binders exhibited values below this threshold, confirming the stiffening influence of nanoparticle addition. Similar findings were reported by [19, 20], showing that nanoparticle modification enhances binder stiffness with reduction in ductility.

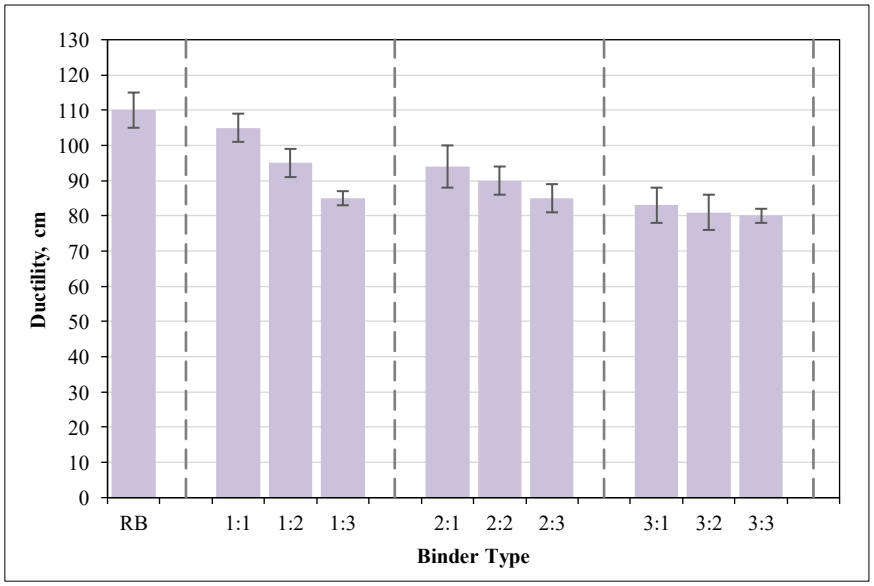

Figure 11. Ductility with different types of binder

As shown in Figure 12, the softening point difference between the top and bottom sections of the stored binders increased gradually with higher nanoparticle contents, ranging from 0.4 °C for RB to 3.1 °C for the (3:3) NT:NZ blend. Although this indicates a slight increase in phase separation tendency, all values remained below the 5 °C limit specified by ASTM D7173, confirming acceptable storage stability. Statistical analysis showed a significant NT×NZ interaction effect ($p = 0.0008$), with binders containing higher NT proportions exhibiting slightly greater differences. This suggests that TiO_2 possess higher bulk density and more tendency to settle during prolonged thermal conditioning, leading to marginally higher softening point variation.

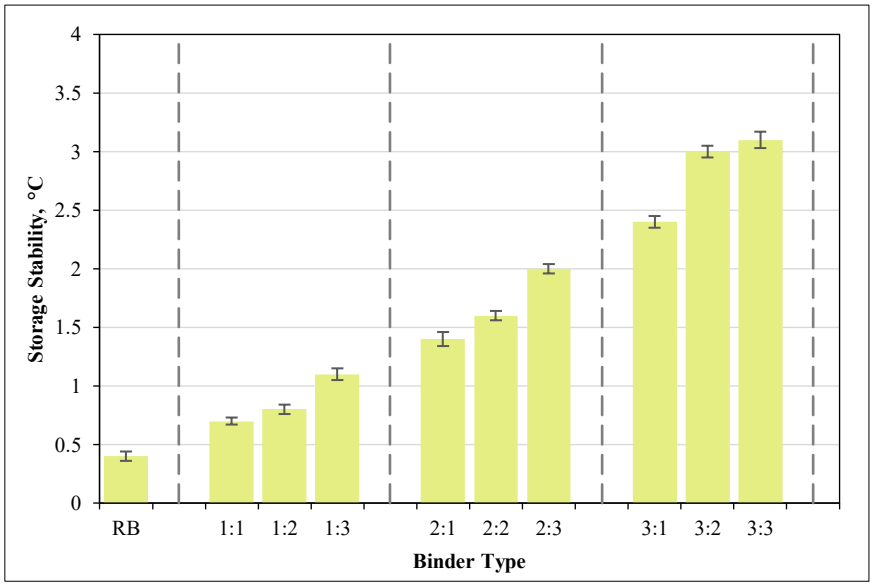

Figure 12. Storage stability with different types of binder

Overall, the incorporation of NT and NZ nanoparticles improved the physical properties of asphalt binders. NZ contributed more to enhancing the softening point and thermal stability, while NT primarily increased stiffness, viscosity, and structural integrity. Their combined use provided a balanced enhancement in stiffness, temperature susceptibility, and workability. However, at higher dosages, such as the (3:3) blend, the binder exhibited greater stiffness accompanied by a reduction in tensile properties (ductility). These results prove a synergistic impact of NT and NZ, which agrees with earlier research [44, 45].

3.2. Results of Aging Performance

The behavior of short-term aging of the asphalt binders modified with nanoparticles was assessed by mass loss and aging indices in terms of penetration, softening point, and viscosity measurements, as shown in Figures 13 and 14. The incorporation of NT and NZ nanoparticles noticeably improved the oxidative stability of the binders compared with the RB. The lowest mass loss was recorded for the (1:3) and (2:3) NT:NZ blends, each showing approximately 0.08%, compared with 0.305% for the RB, representing a reduction of about 74%. This trend suggests that blends containing relatively higher NZ content tend to exhibit lower mass loss values. Statistical analysis confirmed that the combined NT×NZ factor had a significant influence ($p = 0.028$) on mass loss, verifying that the synergistic addition of TiO_2 and ZnO nanoparticles would enhance oxidative resistance. The improvement can be attributed to the nanoparticles' ability to restrict oxygen diffusion and volatilization during RTFO aging, with NZ's higher thermal stability and UV-shielding capacity contributing more effectively to reducing oxidative degradation. Similar conclusions were reported in [22, 46], confirming that ZnO-based nano modifiers are particularly beneficial in enhancing the thermal and oxidative stability of asphalt binders.

Further analysis of the aging indices, as illustrated in Figure 14, demonstrated consistent improvements across all indicators. The penetration aging index (AI_{pen}) decreased from 1.739 for the RB to 1.001 for the (3:3) NT:NZ blend, corresponding to a 42% reduction in hardening. Likewise, the viscosity aging index (AI_{vis}) declined from 1.488 to 0.858, indicating a 42.3% improvement in resistance to viscosity increase. The softening point aging index (AI_{sp}) also showed a smaller but measurable improvement, decreasing from 1.194 to 1.1 (about 7.9% reduction). These findings confirm that nano-modified binders undergo less oxidative hardening during short-term aging than the unmodified binder. Overall, the combined incorporation of TiO_2 and ZnO nanoparticles provided superior aging resistance compared with the RB, primarily due to the synergistic effect of nanoparticle dispersion and their barrier function against oxygen

penetration and thermal degradation. This outcome aligns with earlier studies [30, 33], highlighting the potential of dual-oxide nanomodification in improving the durability and long-term stability of asphalt binders.

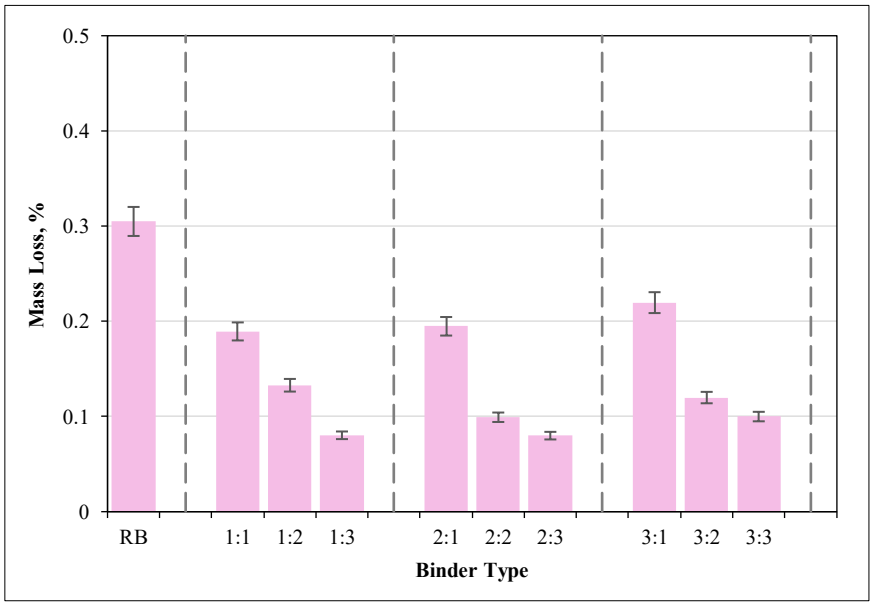

Figure 13. Mass losses with different types of binder

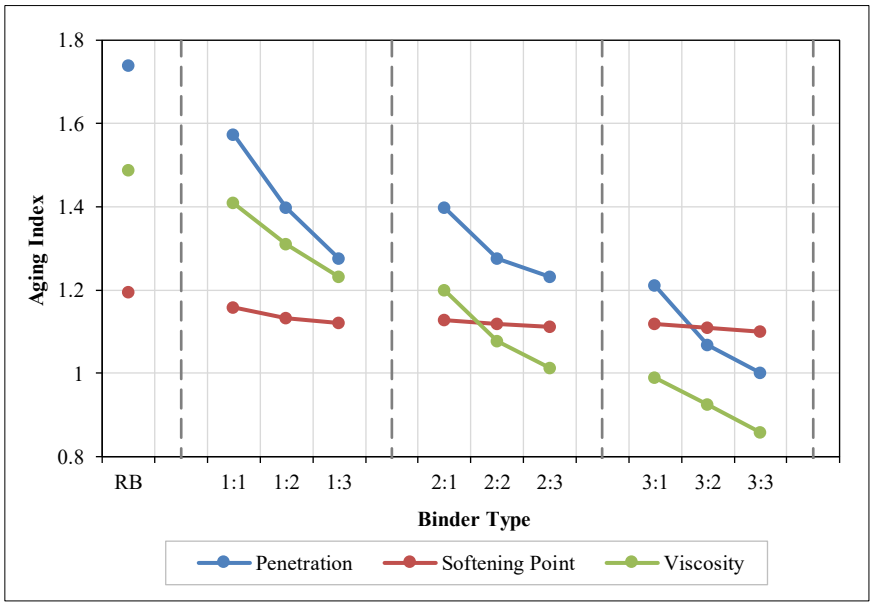

Figure 14. Aging indices with different types of binder

3.3. Results of High-Temperature Performance Grade (PG)

According to AASHTO M320, the rutting parameter (G*/sinδ) used to assess the asphalt binders' high-temperature performance; failure defined as the temperature at which this parameter fell below 1.0 kPa. In comparison to the RB, adding nano titanium dioxide (NT) and nano zinc oxide (NZ) significantly increased binder stiffness and rutting resistance, as seen in Figure 15 and summarized in Table 5.

The RB failed at 74.8 °C with PG 70. It can be observed that lower dosage blends as (1:1) and (1:2) presented slight enhancements with failure temperatures of 74.9 and 75.4 °C recording a PG value of 70. However, high dosages illustrated a notable enhancement in thermal stability with failure temperatures rise from 76.6 °C to 77.9 °C with a PG value of 76.

Blends rich in ZnO (2:3), (3:2), and (3:3), which recorded the greatest G*/sinδ values throughout the tested temperatures, showed the most pronounced benefits. The binder (3:3) showed the highest rutting resistance, failing at 77.9°C, which is about 4% higher than RB. Mixtures (2:3) and (3:2) were closely behind. These results are consistent with rotational viscosity increases presented in (Figure 10), as nanomodified binders showed greater viscosity than RB,

suggesting improved flow resistance and internal cohesion. These rheological results are further supported by higher softening points (Figure 8), since binders with larger softening points are more able to resist deformation in high-temperature service environments.

Mechanically, NZ improves thermal stability and provides UV protection, reducing oxidative degradation and thermal softening, while NT essentially suppress the flexible structure of the bond and cohesion between molecules, enhancing rigidity and structural integrity. These nanoparticles work together to improve the binder's tolerance to high temperatures by reducing molecular motion and maintaining a viscous elastic balance under extended heat [44].

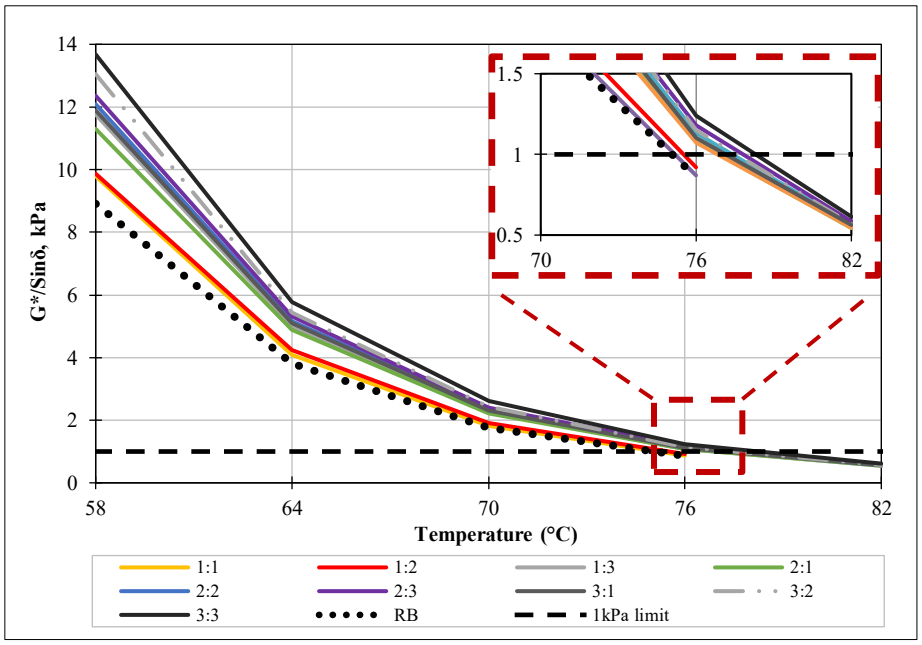

Figure 15. The relation between temperature and variation of G*/sin δ with different types of binder

Table 5. High-temperature performance grade (PG) of the asphalt binders

Binder Type	RB	1:1	1:2	1:3	2:1	2:2	2:3	3:1	3:2	3:3
Fail Temp. °C	74.8	74.9	75.4	76.7	76.6	77.1	77.4	76.9	77.2	77.9
High temp PG	70	70	70	76	76	76	76	76	76	76

The statistical analysis of true failure temperatures confirmed that the combined NT×NZ interaction had a highly significant effect ($p = 0.0008$) on improving the high-temperature performance of the binders. This result verifies that the enhancement in rutting resistance and stiffness arises from the synergistic contribution of both nanoparticles rather than their individual effects. Generally, the dual-oxide system enhances binder rigidity and deformation resistance by restricting molecular mobility and reinforcing the colloidal structure, thereby maintaining viscoelastic stability under elevated temperatures.

Overall, all nano-modified binders outperformed the RB in high-temperature performance. Blends with higher combined doses supporting a higher PG rating of 76 while maintaining the viscosity below the 3,000 MPa limit. The synergistic interaction between TiO_2 and ZnO, especially in balanced or ZnO-rich formulations, has proven to be most effective in improving high-temperature stability and rutting resistance, highlighting their potential as dual oxide nano modifiers to produce more durable asphalt pavements.

3.4. Results of MSCR Test

The results of MSCR at 70 °C are shown in Figure 16 and numerically in Table 6. They highlighted the influences of NT and NZ on rutting (deformation) resistances at two levels of stress: 0.1 and 3.2 kPa. At the lower stress (Figure 15a), all binders exhibited the lowest permanent strain. Nevertheless, at the higher stress of 3.2 kPa (Figure 15b), the differences in binder's behavior became more pronounced, making it easier to assess their resistance to permanent deformation and demonstrate that the nano-modified formulations performed better.

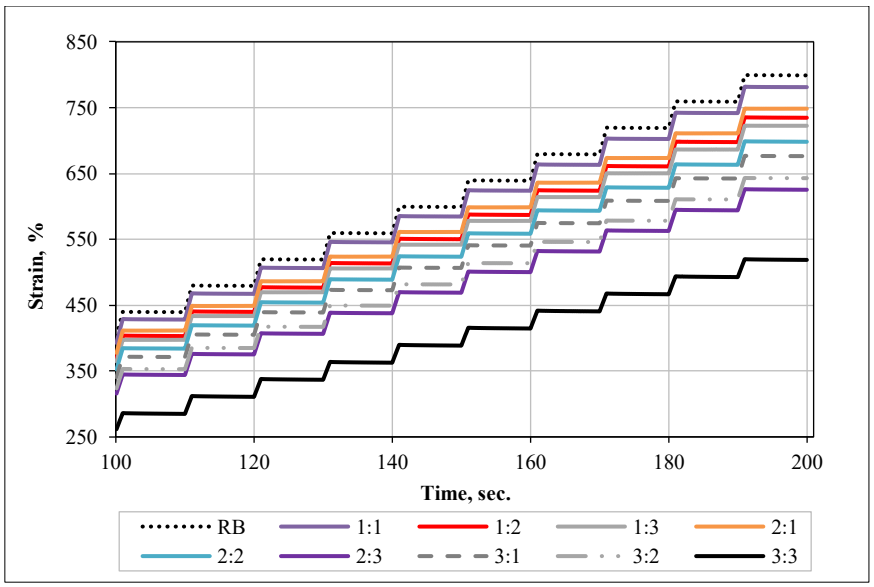

(a)

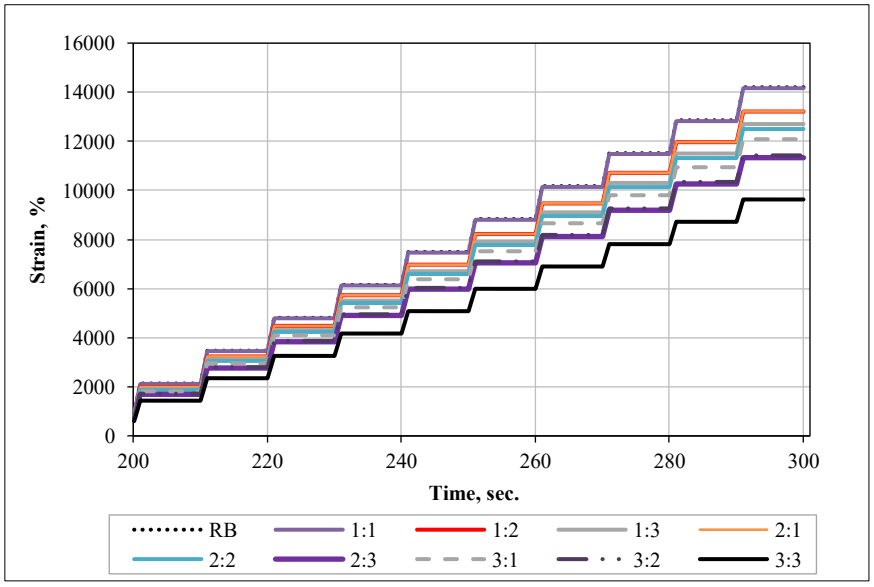

(b)

Figure 16. Creep strain accumulation of the asphalt binders at low (0.1 kPa) and high (3.2 kPa) stress levels

With a high stress level, the RB presented the greatest accumulated creep strain about 14,200%, reflecting its limited rutting resistance and low elastic recovery. However, all binders modified with nanomaterials showed lower strain level suggesting improved permanent deformation because of the inclusion of nanoparticles.

Inclusion of higher nano content showed most of the gains. The 3:3 blend showed cumulative strains of 9,630% corresponding to reductions of approximately 32% compared to the RB. binders with intermediate dosages have confirmed the continued advantages of nanoparticle addition, such as 2:3 and 3:2, which have also shown a reduction of more than 15%. The ability of TiO_2 and ZnO nanoparticles to strengthen the microstructure of the binder by enhancing rigidity and cohesion, which restricts viscous flow and molecular mobility under high shear stress and reduces permanent deformation, is likely the main reason for the enhancement of the rutting resistance.

The assessment of non-recoverable creep ($Jnr_{3.2}$) revealed the observed strain trends, which decrease from 4.139 kPa^{-1} for the RB to 2.834 kPa^{-1} for the 3:3 NT:NZ blend reaching to 31% reduction. However, all modified binders remained within the Standard (S) traffic grade limit ($Jnr_{3.2} \leq 4.5\ kPa^{-1}$) based on AASHTO M332 thus improving resistance to permanent deformation with higher NT and NZ contents. For all formulations, the percentage of elastic recovery ($R_{3.2}$) remained less than 1%, suggesting that stiffening behavior and improved rigidity and flow resistance, rather than elastic rebound, which is the main reasons for the observed improvements in rutting resistance and coincide with past research result [47].

Table 6. Results of MSCR of asphalt binders

Binder type	J_{nr}, kPa^{-1}		R, %	
	0.1 kPa	3.2 kPa	0.1 kPa	3.2 kPa
RB	3.994	4.139	1.18	0.19
1:1	3.92	4.13	3.82	0.41
1:2	3.683	3.86	2.1	0.24
1:3	3.595	3.707	1.22	0.05
2:1	3.72	3.85	1.06	0.16
2:2	3.496	3.662	0.76	0.09
2:3	3.125	3.321	0.46	0
3:1	3.3891	3.532	0.39	0.08
3:2	3.222	3.34	0.20	0
3:3	2.597	2.834	0	0

Statistical analysis confirmed that the NT×NZ interaction had a highly significant effect ($p = 0.000001$) on reducing J_{nr}, demonstrating a strong synergistic improvement in rutting resistance. Individually, both NT ($p = 0.0058$) and NZ ($p = 0.0202$) contributed to this enhancement, with NT exerting a slightly stronger influence through structural reinforcement, while NZ improved nanoparticle dispersion and thermal stability. These findings align with the observed mechanical behavior, where blends with higher NT:NZ ratios (≥ 2:3) exhibited the greatest reductions in cumulative strain and $Jnr_{3.2}$ values.

Overall, the MSCR results confirm that the dual incorporation of TiO_2 and ZnO nanoparticles markedly enhances the high-temperature deformation resistance of asphalt binders. The synergistic interaction between NT and NZ improved binder stability and rutting resistance under elevated temperature and heavy traffic conditions, while all formulations remained within the standard traffic grade limits.

3.5. Results of LAS Test

The LAS results for the assessment of fatigue performance of asphalt binder as characterized using effective shear stress versus shear strain are presented in Figure 17 (a to c). The investigated binder types showed typical viscoelastic behavior with an initial linear increase in stress per unit increment in strain followed by a gradual decrease in post-peak revealing the progressive micro damage accumulation under cyclic loading. The RB showed the least peak stress and a sharp post-peak decrease thus limiting stiffness and reducing capacity to dissipate strain energy. Nevertheless, the modified binders illustrated slightly higher peak stresses and extended strain ranges before failure. This indicates improved ductility and better stress energy absorption. From the results the 1:X formulation and especially the 1:1 and 1:2 blends showed the widest stress and strain curves, highlighting the optimal balance between rigidity and flexibility and suggesting superior fatigue resistance.

Trends in the stress and strain curves are confirmed by fatigue performance data in Table 7. The fatigue life (Nf) of the RB was 50,747 cycles at a 2.5% strain level. On the other hand, 1:1 and 1:2 nano-modified binders showed better fatigue resistance, with NF values of 73,342 and 60,031 cycles, or increases of approximately 45% and 18%, respectively. The increase in elastic recovery (% R) seen in the MSCR test, where the 1:1 and 1:2 blends achieved a recovery of 3.82% and 2.10% at 0.1 kPa, respectively, while the RB achieved only 1.18%, is consistent with these developments. Enhanced elastic recovery indicates improved binder resilience, which delays crack initiation and prolongs fatigue life under low strain level and delays the imitation of the micro crack, these results are well agreed with other researcher studies likes [41].

However, the fatigue life decreased as the nanoparticle content increased, as shown in the 2:X and 3:X series. The 3:3 recorded, for example, only 47,068 cycles. This decrease is probably due to excessive rigidity and agglomeration of nanoparticles, which limits molecular motion and reduces energy dissipation during cyclic stress. Due to the greater deformation and faster deterioration, all asphalt binders had a lower fatigue life at a 5% strain level. However, the 1:1 and 1:2 blends performed better than the RB, getting 3,396 and 2,986 cycles, respectively, as opposed to the 2,403 for the RB.

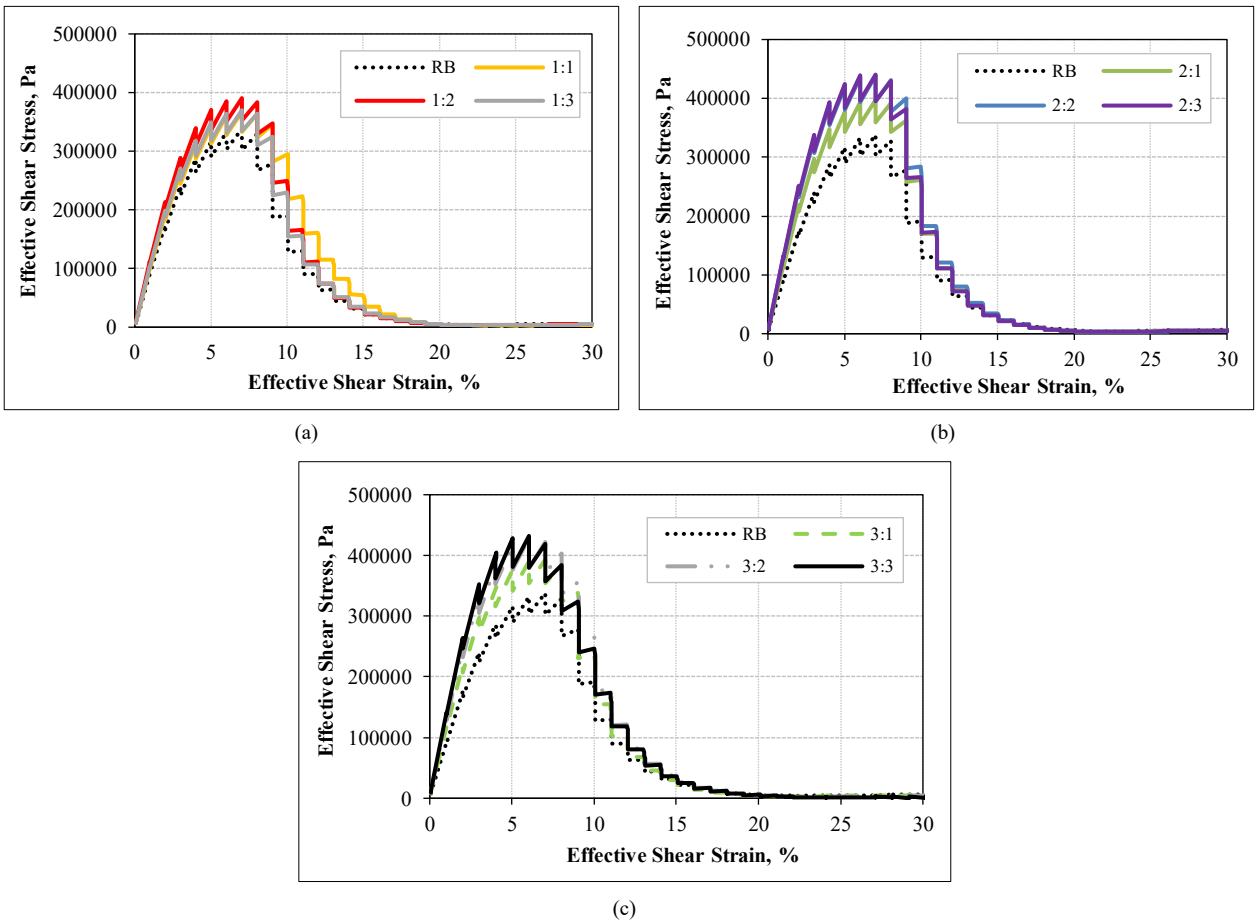

Figure 17. Relationship between effective stress and shear strain for asphalt binders

Table 7. Fatigue life performance of asphalt binders

Binder Type	A	B	Fatigue Life (Nf)	
			2.5%	5%
RB	2.861E+06	4.400	50,747	2,403
1:1	4.259E+06	4.433	73,342	3,396
1:2	3.170E+06	4.329	60,031	2,986
1:3	3.373E+06	4.502	54,513	2,406
2:1	3.323E+06	4.505	53,547	2,358
2:2	3.090E+06	4.495	50,258	2,229
2:3	3.023E+06	4.521	48,027	2,092
3:1	3.426E+06	4.557	52,643	2,236
3:2	2.990E+06	4.494	48,679	2,160
3:3	3.181E+06	4.598	47,068	1,943

Based on the ANOVA results of the NF at a strain level of 2.5%, it's obvious that neither NT nor NZ alone had statistically significant influence (p=0.78 and 0.57, respectively). However, their synergic effect, although exhibiting a p-value that is also higher than 0.05 (0.27), suggests a more noticeable influence on NF. These results align with experimental findings regarding the effective shear stress versus shear strain relationships, which indicate that fatigue resistance is enhanced at intermediate doses (1:1 and 1:2 NT:NZ), and they are consistent with [23, 45]. Overall, the LAS results confirm that, although the nanoparticles strengthen the binder cohesion and delay the initiation appearance of cracking. While excessive additions may compromise flexibility and lead to premature fatigue cracking.

3.6. Economic Evaluation Based on Binder Performance Enhancement

An economic evaluation of the nano-modified asphalt binders was carried out by connecting their metrics of performance improvement with material costs. The unit prices of the base binder (RB) and nanomaterials were taken as

0.27 $/kg (270 $/ton) for RB, 28.5 $/kg (28,500 $/ton) for nano-$TiO_2$ (NT), and 39.4 $/kg (39,400 $/ton) for nano-ZnO (NZ). The total cost of each modified binder was calculated according to the combined NT and NZ dosages.

- The non-recoverable creep compliance (Jnr at 3.2 kPa), representing rutting resistance.
- The fatigue life (Nf at 2.5 % strain) represents flexibility under cyclic loading.
- The viscosity aging index (AI) reflects long-term aging resistance and durability under oxidative conditions.

Because these parameters have opposite desirable trends (lower Jnr and higher Nf indicate better performance), they were normalized to a 0-1 scale to enable direct comparison. For performance indicators where higher values are favorable (e.g., fatigue life), the normalization is performed using:

$$Normalized\ Value = \frac{X - X_{min}}{X_{max} - X_{min}} \quad (7)$$

Conversely, for parameters where lower values are preferable (e.g., Jnr and AI), normalization followed:

$$Normalized\ Value = \frac{X_{max} - X}{X_{max} - X_{min}} \quad (8)$$

An overall performance score then computed by assigning equal weights to the normalized Jnr, Nf and AI values. Finally, the cost-effectiveness index calculated as the ratio between the overall performance score and the total binder cost per ton:

$$\text{Cost-Effectiveness} = \frac{\text{Performance Score}}{\text{Cost per ton}} \quad (9)$$

The results are summarized in Table 8, which presents the total cost, normalized performance indices, and cost-effectiveness for each binder combination.

Table 8. Economic assessment and performance evaluation of nano-enhanced asphalt binders

Binder	Material cost per ton (USD)	Normalized Jnr	Normalized Nf	Normalized AI	Performance Score	Cost-Effectiveness (Score/$)
RB	270	0.000	0.000	0.000	0.000	0.000
1:1	949	0.002	1.000	0.127	0.376	0.000396
1:2	1213	0.068	0.378	0.285	0.244	0.000201
1:3	1477	0.106	0.171	0.403	0.227	0.000154
2:1	1213	0.072	0.149	0.424	0.215	0.000177
2:2	1477	0.138	0.091	0.619	0.283	0.000192
2:3	1741	0.255	0.000	0.728	0.328	0.000188
3:1	1477	0.196	0.067	0.762	0.341	0.000231
3:2	1741	0.233	0.009	0.863	0.368	0.000211
3:3	2307	0.337	0.017	1.000	0.451	0.000195

The results indicate that incorporating the viscosity aging index (AI) allows for a more thorough assessment of binder durability and overall performance. Although adding nanoparticles significantly improved the rheological and mechanical properties of the binder, the economic feasibility is highly dependent on the specific type and dosage of nanoparticles used. Among the tested formulations, the 1:1 binder (1% NT + 1% NZ) exhibited the highest cost-effectiveness (0.000396 Score/$), achieving an optimal balance between improved rutting resistance, fatigue performance, and oxidative aging relative to material expenditure. This formulation reached a score of normalized performance about 0.376, depending on mainly by its excellent fatigue life (Nf = 73,342 cycles), moderate decrement in non-recoverable creep compliance (Jnr = 4.13 kPa^{-1}), and a moderate index of viscosity aging (AI = 1.408).

Although the 3:3 binder showed the minimum Jnr (2.834 kPa^{-1}) and index of viscosity aging (AI = 0.858) thus maintaining superior structural integrity and resistance to aging, its high unit cost (2,307 $/ton) has significantly limited its economic operation. Conversely, lower dosages of binders (1:1 and 1:2) presented stable enhancements through all performance parameters while remaining cost-efficient.

Reviewing the current knowledge to compare nano combined (NT:NZ) as a substitute to used widely and highly accepted material used by many agencies like Styrene Butadiene (SBS) polymer is mostly accepted in the line of binder modification that boosts the performance. Current regional price variations statistics obtained from different local refinery sources refer to that PG76-28 has an initial cost up to $1064 [48] per metric ton using 4% SBS (Kraton SBS-D1192A) as an optimal range content within 40-50 binder. Taking the (1:1) NT and NZ as a baseline for comparison which yield a 949 $. The SBS polymer modified binder may increase the initial RB cost production to 75% as well as

to 11% higher than the initial cost of (1:1) combined nano. Hence, the last modification may be used as an alternative economical solution to enhance binder performance. In summary, the 1:1 nano-modified binder emerges as the most advantageous option both technically and economically, providing an optimal combination of enhanced performance, durability, and affordability, along with strong resistance to rutting, fatigue, and oxidative aging. Balancing 1:1 nano-modified binder as an optimal combined content which considered as the best option in terms of technical and economic advantages where the perfect integration improved the performance, durability, and affordability that led to resist fatigue and oxidative aging.

4. Conclusions

Several advantages of using a single type of nanomaterial were recorded in literature, though the simultaneous use of two types (NT and NZ) has received little attention and thereby been investigated during the course of this research. The dosages investigated range from 1% to 3% (by weight of asphalt binder) with an increment rate of 1%. So, 9 different combinations were used to modify the asphalt binder. The conducted tests for performance evaluation include physical, aging, rheological, rutting, and fatigue resistance. The following conclusions were drawn based on the laboratory testing program:

- A noticeable increase in binder stiffness was observed with increasing dosages of nanomaterial. The combined use of NT and NZ with high dosages (3%) leads to a decrease of 50%, an increase of 12% and 81.5 % as compared to the reference binder for penetration, softening point, and viscosity tests, respectively.
- Short-term aging resistance improved due to the synergistic interaction of NT and NZ. Aging indices based on penetration and viscosity indicated that NT had a stronger influence on hardening control, whereas NZ contributed more effectively to oxidative resistance through enhanced thermal stability at the softening point.
- There is a general trend for improving the high-temperature PG of asphalt binder modified with NT and NZ, as compared with the reference binder, which has a PG grade of 70°C, all the modified binders have a corresponding PG grade of 76 °C, except the 1:1 and 1:2 combinations.
- As compared to the limited resistance to permanent deformation of the RB demonstrated in the MSCR test, both NT and NZ significantly improved the resistance as indicated by the Jnr values ($p < 0.05$), with NT showing a slightly stronger effect. The blend of (3:3) showed a 31% reduction in Jnr3.2. It achieved a value of 2.834 kPa^{-1} in comparison to RB with a value of 4.139 kPa^{-1}.
- The highest fatigue resistance as indicated from the LAS test, showed that the blend with 1% NT and NZ has the longest fatigue life (NF). It recorded NF of 73,342 cycles at a 2.5 strain level in comparison to 50,747 cycles for RB. A higher dosage, like (2:2), (3:2) or (3:3) reveals a negative effect on NF.
- Cost- performance analysis revealed that the blend (1:1) is the most recommended blend due to its superior resistance to fatigue cracking, improved resistance to rutting, and balanced increase in cost.
- Based on the findings of this study, a combined use of NT and NZ with 1% for each one, i.e., (1 % NT + 1 % NZ) is recommended. However, this study was limited to laboratory scale testing under controlled conditions. Field verification is necessary to confirm practical applicability for the recommended dosage.

4.1. Future Research

Future investigations could extend beyond the current rheological and physical evaluation of NT and NZ to explore the fundamental physicochemical interactions governing their synergistic behavior within asphalt binders. Advanced nanoscale characterization techniques are recommended to directly assess the morphology, dispersion, and bonding mechanisms of these nanomaterials within the binder matrix. Techniques such as Scanning Electron Microscopy (SEM) and X-ray Diffraction (XRD) can be employed to examine structural configurations and phase distributions, while Atomic Force Microscopy (AFM) may provide insights into nanoscale surface interactions. Additionally, Fourier Transform Infrared Spectroscopy (FTIR) could be utilized to identify chemical functional groups and evaluate the molecular compatibility of TiO_2–ZnO nanocomposites with asphalt constituents. Such studies will provide a deeper understanding of nano–binder interactions and contribute to the advancement of nanomodified asphalt binders.

5. Declarations

5.1. Author Contributions

Conceptualization, A.A.; methodology, A.A. and H.O.; software, H.K.M.; validation, A.A. and H.O.; formal analysis, A.A. and H.O.; investigation, A.A.; resources, A.A. and H.O.; data curation, A.A. and H.O.; writing—original draft preparation, A.A. and H.K.M.; writing—review and editing, H.O.; visualization, A.A. and H.K.M.; supervision, A.A.; project administration, A.A.; funding acquisition, A.A., H.O., and H.K.M. All authors have read and agreed to the published version of the manuscript.

5.2. Data Availability Statement

The data presented in this study are available in the article.

5.3. Funding

The authors received no financial support for the research, authorship, and/or publication of this article.

5.4. Conflicts of Interest

The authors declare no conflict of interest.

6. References

[1] Zhang, H., Yu, J., Wang, H., & Xue, L. (2011). Investigation of microstructures and ultraviolet aging properties of organo-montmorillonite/SBS modified bitumen. Materials Chemistry and Physics, 129(3), 769–776. doi:10.1016/j.matchemphys.2011.04.078.

[2] Yang, Q., Liu, Q., Zhong, J., Hong, B., Wang, D., & Oeser, M. (2019). Rheological and micro-structural characterization of bitumen modified with carbon nanomaterials. Construction and Building Materials, 201, 580–589. doi:10.1016/j.conbuildmat.2018.12.173.

[3] Li, R., Xiao, F., Amirkhanian, S., You, Z., & Huang, J. (2017). Developments of nano materials and technologies on asphalt materials – A review. Construction and Building Materials, 143, 633–648. doi:10.1016/j.conbuildmat.2017.03.158.

[4] Hamid, A., Baaj, H., & El-Hakim, M. (2023). Temperature and Aging Effects on the Rheological Properties and Performance of Geopolymer-Modified Asphalt Binder and Mixtures. Materials, 16(3), 1012. doi:10.3390/ma16031012.

[5] Adnan, A. M., & Wang, J. (2025). Rheological and storage stability improvement of SBR modified asphalt binder using graphene. Road Materials and Pavement Design, 1–23. doi:10.1080/14680629.2025.2523397.

[6] Taherkhani, H., Afroozi, S., & Javanmard, S. (2017). Comparative Study of the Effects of Nanosilica and Zyco-Soil Nanomaterials on the Properties of Asphalt Concrete. Journal of Materials in Civil Engineering, 29(8), 4017054. doi:10.1061/(asce)mt.1943-5533.0001889.

[7] Tanzadeh, J., & Otadi, A. (2018). Testing and evaluating the effect of adding fibers and nanomaterials on improving the performance properties of thin surface asphalt. Journal of Testing and Evaluation, 47(1), 654–677. doi:10.1520/JTE20170409.

[8] Karki, B., Berg, A., Saha, R., Melaku, R. S., & Gedafa, D. S. (2018). Effect of Nanomaterials on Binder Performance. International Conference on Transportation and Development 2018, 332–338. doi:10.1061/9780784481554.034.

[9] Ganesh, K., & Prajwal, D. T. (2020). Studies on fatigue performance of modified dense bituminous macadam mix using nano silica as an additive. International Journal of Pavement Research and Technology, 13(1), 75–82. doi:10.1007/s42947-019-0087-z.

[10] Albayati, A. H., Latief, R. H., Al-Mosawe, H., & Wang, Y. (2024). Nano-Additives in Asphalt Binder: Bridging the Gap between Traditional Materials and Modern Requirements. Applied Sciences (Switzerland), 14(10), 3998. doi:10.3390/app14103998.

[11] Albayati, A. H., Al-Ani, A. F., Byzyka, J., Al-Kheetan, M., & Rahman, M. (2024). Enhancing Asphalt Performance and Its Long-Term Sustainability with Nano Calcium Carbonate and Nano Hydrated Lime. Sustainability (Switzerland), 16(4), 1507. doi:10.3390/su16041507.

[12] Bica, B. O., & de Melo, J. V. S. (2020). Concrete blocks nano-modified with zinc oxide (ZnO) for photocatalytic paving: Performance comparison with titanium dioxide (TiO2). Construction and Building Materials, 252, 119120. doi:10.1016/j.conbuildmat.2020.119120.

[13] Huang, H., Wang, Y., Wu, X., Zhang, J., & Huang, X. (2024). Nanomaterials for Modified Asphalt and Their Effects on Viscosity Characteristics: A Comprehensive Review. Nanomaterials, 14(18), 1503. doi:10.3390/nano14181503.

[14] Lima, O., Afonso, C., Segundo, I. R., Landi, S., Homem, N. C., Freitas, E., Alcantara, A., Branco, V. C., Soares, S., Soares, J., Teixeira, V., & Carneiro, J. (2022). Asphalt Binder "Skincare"? Aging Evaluation of an Asphalt Binder Modified by Nano-TiO2. Nanomaterials, 12(10), 1678. doi:10.3390/nano12101678.

[15] Hu, Z., Xu, T., Liu, P., & Oeser, M. (2021). Developed photocatalytic asphalt mixture of open graded friction course for degrading vehicle exhaust. Journal of Cleaner Production, 279, 123453. doi:10.1016/j.jclepro.2020.123453.

[16] Rondón-Quintana, H. A., Ruge-Cárdenas, J. C., & Zafra-Mejía, C. A. (2023). The Use of Zinc Oxide in Asphalts: Review. Sustainability, 15(14), 11070. doi:10.3390/su151411070.

[17] Haghshenas, H. F., Rea, R., & Haghshenas, D. F. (2019). Aging resistance of asphalt binders through the use of zinc diethyldithiocarbamate. Petroleum Science and Technology, 37(22), 2275–2282. doi:10.1080/10916466.2019.1633348.

[18] Zhang, H., Zhu, C., & Kuang, D. (2016). Physical, Rheological, and Aging Properties of Bitumen Containing Organic Expanded Vermiculite and Nano-Zinc Oxide. Journal of Materials in Civil Engineering, 28(5), 4015203. doi:10.1061/(asce)mt.1943-5533.0001499.

[19] Tanzadeh, J., Vahedi, F., Pezhouhan, T. K., & Tanzadeh, R. (2013). Laboratory study on the effect of nano Tio2 on rutting performance of asphalt pavements. Advanced Materials Research, 622, 990–994. doi:10.4028/www.scientific.net/AMR.622-623.990.

[20] Buhari, R., Abdullah, M. E., Ahmad, M. K., Chong, A. L., Haini, R., & Abu Bakar, S. K. (2018). Physical and rheological properties of Titanium Dioxide modified asphalt. E3S Web of Conferences, 34. doi:10.1051/e3sconf/20183401035.

[21] Qian, G., Yu, H., Gong, X., & Zhao, L. (2019). Impact of Nano-TiO2 on the NO2 degradation and rheological performance of asphalt pavement. Construction and Building Materials, 218, 53–63. doi:10.1016/j.conbuildmat.2019.05.075.

[22] Dell'Antonio Cadorin, N., Victor Staub de Melo, J., Borba Broering, W., Luiz Manfro, A., & Salgado Barra, B. (2021). Asphalt nanocomposite with titanium dioxide: Mechanical, rheological and photoactivity performance. Construction and Building Materials, 289, 123178. doi:10.1016/j.conbuildmat.2021.123178.

[23] Ameli, A., Hossein Pakshir, A., Babagoli, R., Norouzi, N., Nasr, D., & Davoudinezhad, S. (2020). RETRACTED: Experimental investigation of the influence of Nano TiO2 on rheological properties of binders and performance of stone matrix asphalt mixtures containing steel slag aggregate. Construction and Building Materials, 265, 120750. doi:10.1016/j.conbuildmat.2020.120750.

[24] Weigel, S., Simnofske, D., Rückert, P., Stephan, D., Mollenhauer, K., & Dudenhöfer, B. (2020). Effects of Titanium Dioxide on the Structure and Properties of Bitumen. Journal of Materials in Civil Engineering, 32(3), 4020001. doi:10.1061/(asce)mt.1943-5533.0003074.

[25] Aboelmagd, A. Y., Moussa, G. S., Enieb, M., Khedr, S., & Alla, E. S. M. A. (2021). Evaluation of Hot Mix Asphalt and Binder Performance Modified with High Content of Nano Silica Fume. Journal of Engineering Sciences, 49(4), 378–399. doi:10.21608/jesaun.2021.70733.1046.

[26] Tavares Marinho Filho, P. G., De Figueirêdo Lopes Lucena, L. C., & Costa Lopes, M. (2022). Investigation of titanium nanoparticles-reinforced Asphalt Composites Using Rheological Tests. Transportes, 30(2), 2614. doi:10.14295/transportes.v30i2.2614.

[27] Enieb, M., Cengizhan, A., Karahancer, S., & Eltwati, A. (2023). Evaluation Of Physical-Rheological Properties of Nano Titanium Dioxide Modified Asphalt Binder and Rutting Resistance of Modified Mixture. International Journal of Pavement Research and Technology, 16(2), 285–303. doi:10.1007/s42947-021-00131-0.

[28] Mohammed, A. M., & Abed, A. H. (2024). Effect of nano-TiO2 on physical and rheological properties of asphalt cement. Open Engineering, 14(1), 20220520. doi:10.1515/eng-2022-0520.

[29] Albayati, A. H., Oukaili, N. K., Moudhafar, M. M., Allawi, A. A., Said, A. I., & Ibrahim, T. H. (2024). Experimental Study to Investigate the Performance-Related Properties of Modified Asphalt Concrete Using Nanomaterials Al2O3, SiO2, and TiO2. Materials, 17(17), 4279. doi:10.3390/ma17174279.

[30] Zhang, H., Gao, Y., Guo, G., Zhao, B., & Yu, J. (2018). Effects of ZnO particle size on properties of asphalt and asphalt mixture. Construction and Building Materials, 159, 578–586. doi:10.1016/j.conbuildmat.2017.11.016.

[31] Yunus, K. N. M., Zainorabidin, A., Kamaruddin, N. H. M., Ahmad, M. K., Anuar, N. F. N., & Yaakop, S. N. K. (2022). Physical and Chemical Properties of Nano Zinc Oxide Modified Asphalt Binder. International Journal of Integrated Engineering, 14(9), 133–139. doi:10.30880/ijie.2022.14.09.017.

[32] Saltan, M., Terzi, S., & Karahancer, S. (2019). Mechanical Behavior of Bitumen and Hot-Mix Asphalt Modified with Zinc Oxide Nanoparticle. Journal of Materials in Civil Engineering, 31(3), 4018399. doi:10.1061/(asce)mt.1943-5533.0002621.

[33] Xu, X., Guo, H., Wang, X., Zhang, M., Wang, Z., & Yang, B. (2019). Physical properties and anti-aging characteristics of asphalt modified with nano-zinc oxide powder. Construction and Building Materials, 224, 732–742. doi:10.1016/j.conbuildmat.2019.07.097.

[34] Kleizienė, R., Paliukaitė, M., & Vaitkus, A. (2020). Effect of Nano SiO2, TiO2 and ZnO Modification to Rheological Properties of Neat and Polymer Modified Bitumen. Proceedings of the 5th International Symposium on Asphalt Pavements & Environment (APE). ISAP APE 2019. Lecture Notes in Civil Engineering, vol 48. Springer, Cham, Switzerland. doi:10.1007/978-3-030-29779-4_32.

[35] Neto, V. F. de S., Lucena, L. C. de F. L., de Barros, A. G., Lucena, A. E. de F. L., & Filho, P. G. T. M. (2022). Rheological evaluation of asphalt binder modified with zinc oxide nanoparticles. Case Studies in Construction Materials, 17, 1224. doi:10.1016/j.cscm.2022.e01224.

[36] Kamboozia, N., Mousavi Rad, S., & Saed, S. A. (2022). Laboratory Investigation of the Effect of Nano-ZnO on the Fracture and Rutting Resistance of Porous Asphalt Mixture under the Aging Condition and Freeze–Thaw Cycle. Journal of Materials in Civil Engineering, 34(5), 4022052. doi:10.1061/(asce)mt.1943-5533.0004187.

[37] Al-Mistarehi, B., Al-Omari, A., Taamneh, M., Imam, R., & Al-Deen Khafaja, D. (2023). The effects of adding nano clay and nano zinc oxide on asphalt cement rheology. Journal of King Saud University - Engineering Sciences, 35(4), 260–269. doi:10.1016/j.jksues.2021.03.010.

[38] Staub de Melo, J. V., Manfro, A. L., Barra, B. S., Dell'Antonio Cadorin, N., & Borba Broering, W. (2023). Evaluation of the Rheological Behavior and the Development of Performance Equations of Asphalt Composites Produced with Titanium Dioxide and Zinc Oxide Nanoparticles. Nanomaterials, 13(2), 288. doi:10.3390/nano13020288.

[39] Zhu, Q., He, Z., Wang, J., & Wang, S. (2024). Morphology, rheology and physical properties investigations of multi-scale nano-zinc oxide modified asphalt binder. Alexandria Engineering Journal, 89, 31–38. doi:10.1016/j.aej.2023.12.031.

[40] Fu, Z., Tang, Y., Ma, F., Wang, Y., Shi, K., Dai, J., Hou, Y., & Li, J. (2022). Rheological properties of asphalt binder modified by nano-TiO2/ZnO and basalt fiber. Construction and Building Materials, 320, 126323. doi:10.1016/j.conbuildmat.2022.126323.

[41] Di, H., Zhang, H., Yang, E., Ding, H., Liu, H., Huang, B., & Qiu, Y. (2023). Usage of Nano-TiO2 or Nano-ZnO in Asphalt to Resist Aging by NMR Spectroscopy and Rheology Technology. Journal of Materials in Civil Engineering, 35(1), 4022391. doi:10.1061/(asce)mt.1943-5533.0004570.

[42] Han, D., Hu, G., & Zhang, J. (2023). Study on Anti-Aging Performance Enhancement of Polymer Modified Asphalt with High Linear SBS Content. Polymers, 15(2), 256. doi:10.3390/polym15020256.

[43] Shafabakhsh, G. A., Sadeghnejad, M., Ahoor, B., & Taheri, E. (2020). Laboratory experiment on the effect of nano SiO2 and TiO2 on short and long-term aging behavior of bitumen. Construction and Building Materials, 237, 117640. doi:10.1016/j.conbuildmat.2019.117640.

[44] Al-Hamdou, Y. M., & Albayati, A. H. (2025). The Influence of Nanomaterials on the Permanent Deformation of Hot Mix Asphalt. Engineering, Technology & Applied Science Research, 15(4), 25538–25544. doi:10.48084/etasr.12244.

[45] Al-Hamdou, A. M., & Albayati, A. H. (2025). Fatigue performance of asphalt binders modified with varying nanomaterials. Results in Engineering, 28. doi:10.1016/j.rineng.2025.107238.

[46] An, B., Shen, Y., Liu, J., Li, J., Jing, H., & Ren, S. (2025). Anti-Aging Effect of Nano-ZnO on Asphalt: Chemo-Rheological Behavior, Molecular Size Evolution of Polymers, and Nanoscale Parameters. Polymers, 17(20), 2774. doi:10.3390/polym17202774.

[47] Zhao, S., You, Q., Ling, J., Zhang, J., Chineche, E. B., & Wang, J. (2024). Variation of nano-ZnO/SBR modified asphalt features under photo-oxidative aging and optimization of the evaluation indexes based on rheological properties and chemical structure. Case Studies in Construction Materials, 21, 4101. doi:10.1016/j.cscm.2024.e04101.

[48] Hossain, Z., Zaman, M., Hawa, T., & Saha, M. C. (2015). Evaluation of Moisture Susceptibility of Nanoclay-Modified Asphalt Binders through the Surface Science Approach. Journal of Materials in Civil Engineering, 27(10). doi:10.1061/(asce)mt.1943-5533.0001228.